Collisionally Aided Coherent Emission at an Optical Frequency

E. Giacobino and P. R. Berman[a]

Laboratoire de Spectroscopie Hertzienne de l'Ecole Normale Supérieure, 75252 Paris Cedex 05, France

(Received 3 October 1986)

Experimental evidence is presented for collisionally aided excitation of $4D$-$3P_{3/2}$ electronic-state, optical coherence in Na. A simple theoretical model of the reaction is proposed which gives agreement with experiment.

PACS numbers: 34.50.Rk, 32.80.−t, 42.65.−k

With the development of high-power laser sources, it has become possible to study a new class of collisional radiative reactions. Theoretical and experimental studies of such collisionally aided reactions, which require a collision and external radiation field to act simultaneously, were initially aimed at calculating or measuring the overall initial- to final-state cross sections.[1] Subsequently, it became appreciated that such reactions can also produce coherence among degenerate magnetic sublevels.[2] In a parallel development,[3] a series of experiments was carried out in which a collisionally aided excitation of a coherence between the *nondegenerate* $3P_{1/2}$ and $3P_{3/2}$ states of Na was generated.

The above studies of collisionally aided excitation of atomic coherence were limited to coherence between levels within the same electronic manifold. It was shown theoretically[4] that one should also be able to produce collisionally aided coherence between different electronic levels. If such a coherence is created between states of opposite parity, it can lead to coherent emission at the atomic transition frequency associated with these levels.

In this work, we present experimental evidence for a collisionally aided excitation of the $4D$-$3P_{3/2}$ electronic-state, optical coherence in Na produced via the reaction (Fig. 1)

$$\mathrm{Na}(3S_{1/2})+\mathrm{He}+\hbar\Omega_1+2\hbar\Omega_2\rightarrow\mathrm{Na}(4D,3P_{3/2})+\mathrm{He}, \tag{1}$$

in which the notation $(4D,3P_{3/2})$ indicates a coherent superposition of the $4D$ and $3P_{3/2}$ states. The frequencies Ω_1 and $2\Omega_2$ are detuned by several wave numbers from the $3S$-$3P_{3/2}$ and $3S$-$4D$ transitions, respectively. The frequency Ω_1 is held fixed as Ω_2 is varied. When the detuning for the two-photon ($3S$-$4D$) transition is equal to that for the one-photon ($3S$-$3P_{3/2}$) transition, a resonant structure is seen if one monitors emission from the sample at the $4D$-$3P_{3/2}$ transition frequency (Figs. 1 and 2). This resonant structure *is not present in the absence of collisions* and, as is discussed below, is evidence for the creation of collisionally aided $4D$-$3P_{3/2}$ electronic-state coherence in Na. It will also be seen that the coherence time associated with the pulsed laser sources plays an important role in the excitation process.[5]

A qualitative interpretation of the results can be made by calculating the polarization of the sample in lowest-order perturbation theory, assuming cw laser fields. The component of the polarization which is relevant to our discussion is the one that oscillates at frequency $2\Omega_2-\Omega_1$. This component of the polarization is directly related to a density matrix element ρ_{21}, which, in lowest-order perturbation theory, can be calculated from the optical Bloch equations as

$$\rho_{21}^{(3)}(2\Omega_2-\Omega_1)=(\chi_2\chi_2'/\Delta)\chi_1^*\exp\{i[(2\mathbf{k}_2-\mathbf{k}_1)\cdot\mathbf{R}-(2\Omega_2-\Omega_1)t]\}\frac{1}{\delta_1\delta_2}\left[\frac{1}{f}+\frac{\Gamma}{\Gamma_{21}-i(\delta_2-\delta_1)}\right], \tag{2}$$

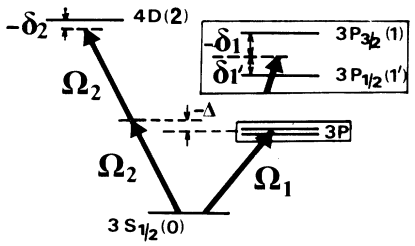

FIG. 1. Energy-level diagram for Na; the $4D$ fine structure and all the hyperfine structures are not resolved in the experiment. The numbers in parentheses are state labels used in the text.

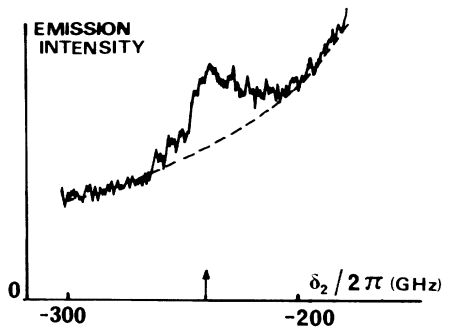

FIG. 2. Experimental curve of emission intensity (arbitrary units) at $\lambda=560$ nm in the direction $2\mathbf{k}_2-\mathbf{k}_1$ as a function of $\delta_2/2\pi$ for $\delta_1/2\pi=-240$ GHz and $P_{\mathrm{He}}=140$ Torr.

where

$$\Gamma=\Gamma_{20}+\Gamma_{01}-\Gamma_{21}; \quad 1/f=1+(\delta_1/2\delta_1'). \tag{3}$$

The indices 0, 1, 1', and 2 refer to states $3S_{1/2}$, $3P_{3/2}$, $3P_{1/2}$, and $4D$ respectively; the χ's are the Rabi frequencies associated with the fields, $\chi_i=\mathbf{E}_i\cdot\mathbf{d}_{01}/2\hbar$, $\chi_2'=\mathbf{E}_2\cdot\mathbf{d}_{12}/2\hbar$ (E_i, Ω_i, and $\mathbf{k}_i$ are the amplitude, frequency, and propagation vector of field i; $\mathbf{d}_{ij}$ is a dipole moment element). The detunings are defined as $\delta_1=\Omega_1-\omega_{10}$, $\delta_2=\Omega_2-\omega_{20}$, $\delta_1'=\Omega_1-\omega_{1'0}$, and $\Delta=\omega_{10}-\Omega_2$; the Γ_{ij}'s are the (complex) collisional decay rates associated with the ij atomic-state coherence. The quantity $\chi_2^{\mathrm{TP}}=\chi_2\chi_2'/\Delta$ plays the role of an effective two-photon Rabi frequency. In deriving Eq. (2), we have assumed that $|\Delta| \gg |\delta_1|$, $|\delta_2| \gg \Gamma_{ij} \gg$ all Doppler widths $\gg$ all spontaneous decay rates. The last two inequalities, which are *not* valid at low perturber pressure ($P_{\mathrm{He}}<30$ Torr), explain why various Doppler shifts and spontaneous decay rates do not appear in Eq. (2).

Equation (2) is analogous to the one given by Bloembergen and co-workers[3] for the creation of a coherence between two levels having the same parity. Two terms contribute to $\rho_{12}^{(3)}(2\Omega_2-\Omega_1)$. The first term in brackets in Eq. (2) has as its origin a four-wave mixing process. This term is pressure independent (it exists even in the absence of collisions) and does *not* have a resonant structure in the region $\delta_2\simeq\delta_1$.[6] Both the $3P_{3/2}$ and $3P_{1/2}$ states can serve as intermediate states in the four-wave-mixing interaction, which is why both detunings δ_1 and δ_1' appear in the factor f. The second term in brackets in Eq. (2) vanishes in the absence of collisions and *does* have a resonant structure when $\delta_2\simeq\delta_1$; the contribution from the $3P_{1/2}$ state in the vicinity of the resonance is negligible.

A fifth-order contribution[7] to ρ_{21}, arising from the collisionally aided excitation of the $3P_{3/2}$ level followed by a four-wave-mixing process, can be neglected, provided that $|\chi_1|^2<\gamma_1|\delta_1|$, where γ_1 is the $3P$ spontaneous decay rate.

Since levels 1 and 2 are of opposite parity, an electric dipole coherence associated with ρ_{21} is expected to give rise to emission in the direction $\mathbf{k}_s=2\mathbf{k}_2-\mathbf{k}_1$ with an intensity I proportional to

$$I\propto|\rho_{21}(2\Omega_2-\Omega_1)|^2 = \frac{|\chi_2^{\mathrm{TP}}\chi_1|^2}{\delta_1^2\delta_2^2 f^2}\left[1+\frac{\{2yf+(yf)^2\}\Gamma_{21}^2}{\Gamma_{21}^2+(\delta_2-\delta_1)^2}\right], \tag{4}$$

where $y=\Gamma/\Gamma_{21}$ and all collisional shifts have been neglected (Γ_{ij}'s taken as real). Equation (4) is to be compared with the experimental profiles.

The experimental arrangement that was used to obtain Fig. 2 is shown schematically in Fig. 3. Two yttrium-aluminum-garnet–pumped dye lasers with wavelengths approximately equal to 589 nm (Ω_1) and 579 nm (Ω_2), respectively, are sent with crossed polarizations into a heat-pipe containing sodium vapor and helium buffer gas. The sodium density is in the range 10^{13}–10^{14} atoms/cm^3; the helium pressure can be varied from one Torr to several hundred Torr. The two laser beams overlap in the heat pipe, making an angle of a few milliradians. A lens focuses the emerging signal on a pinhole located in the direction $\mathbf{k}_s$. This design eliminates most of the background lasers' light. Additional filtering of the signal is provided by a polarizer which eliminates the remaining light at frequency Ω_2 (the polarization of the signal beam is expected to be parallel to that of the beam at Ω_1) and by an interference filter centered on 568 nm. The signal is monitored with a photomultiplier followed by a boxcar integrator.

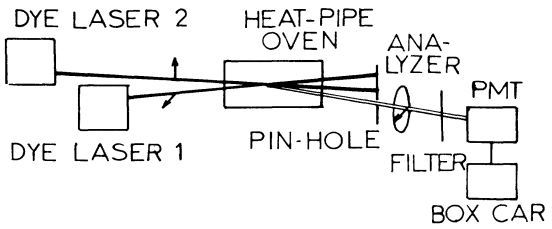

FIG. 3. Experimental setup.

Phase matching is achieved by using a detuning $\delta_1<0$. For $\delta_1<0$, the beam at frequency Ω_1 sees an index of refraction larger than unity, because of its interaction with the Na atoms (the change in index for the other field and the signal field can be neglected). With this change in index, the phase-matching conditions $\mathbf{k}_s=2\mathbf{k}_2-\mathbf{k}_1$, $\Omega_s=2\Omega_2-\Omega_1$ can be achieved with a small angle between $\mathbf{k}_1$ and $\mathbf{k}_2$.[8] At a fixed helium pressure, the value of sodium density and δ_1 (which both modify the index change) are varied to achieve a maximum in phase matching (detected as a maximum in the nonresonant background emission for some fixed value of δ_2). With this value of δ_1 kept fixed, the detuning δ_2 is slowly scanned as the signal (averaged over many laser pulses) is recorded.

A typical curve is shown in Fig. 2. The expected collisionally aided Lorentzian emission profile centered at $\delta_2=\delta_1$ can be seen superimposed on a background which can be reasonably well approximated with a δ_2^{-2} dependence. These curves were obtained with Rabi frequencies $\chi_1/2\pi\simeq0.7$ GHz and $\chi_2^{\mathrm{TP}}/2\pi\simeq10$ MHz (the condition for neglect of the fifth-order contribution is $\chi_1/2\pi<2$GHz). A dispersive structure, characteristic of the higher-order terms, is seen when $\chi_1/2\pi$ was increased to 2.5 GHz.

The ratio r of the resonant signal component to the nonresonant background at $\delta_2=\delta_1$ as a function of pressure is shown in Fig. 4. Although the data were taken with different detunings δ_1, the results are corrected to an equivalent detuning $\delta_1/2\pi=-255$ GHz for each point. This ratio increases with pressure and then saturates. In attempting to compare the experimental results with theoretical expression (4), one immediately encounters dif-

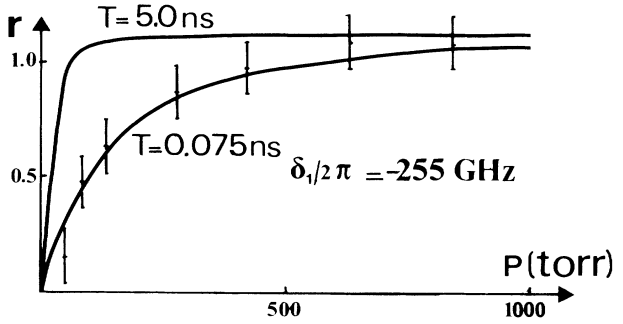

FIG. 4. Experimental points (with error bars) and theoretical curves of the ratio r of signal to background at $\delta_{21}=(\delta_2-\delta_1)=0$ as a function of helium pressure P. A ratio $y=\Gamma/\Gamma_{21}=0.23$ is assumed for the theoretical curves.

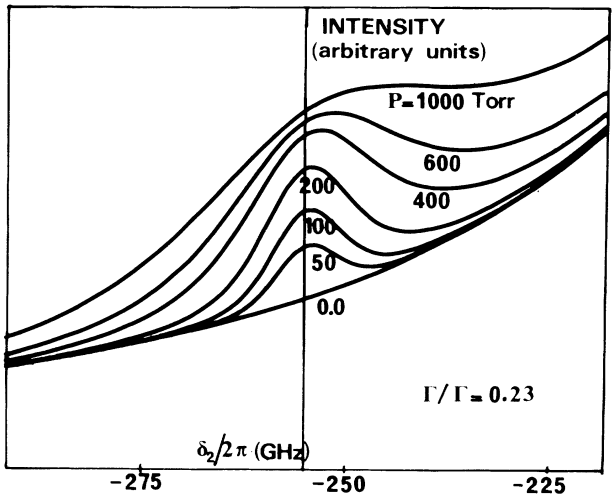

FIG. 5. Theoretical curves of emission intensity (arbitrary units) as a function of detuning $\delta_2/2\pi$ for $\delta_1/2\pi=-255$ GHz and $T=0.075$ ns. Each curve is labeled by the helium pressure P in Torr.

ficulties. Equation (4) predicts a *constant* value $r=2yf+(yf)^2$ which is inconsistent with the low-pressure data.

In order to explain the differences between the cw theory and experiment, we have carried out a calculation assuming laser fields with Gaussian temporal pulse envelope functions. The corresponding Rabi frequencies are given by $\chi_1(t_1)=\chi_1\exp(-t_1^2/T^2)$; $\chi_2^{\rm TP}(t_2)=\chi_2^{\rm TP}\times\exp(-2t_2^2/T^2)$, where $t_i=t-\mathbf{k}_i\cdot\mathbf{R}/c$. Assuming that $|\delta_1|T\gg1$, $|\delta_2|T\gg1$, and that the medium is optically thin, one can show that, in terms of the density matrix element $\rho_{21}(\mathbf{R},t)$, the integrated signal intensity emitted in the direction $\mathbf{k}_s$ is proportional to $I\equiv\int_{-\infty}^{\infty}|\langle\rho_{21}(\mathbf{R},t)\rangle|^2dt$ given by

$$I=\frac{|\chi_2^{\rm TP}\chi_1|^2}{\delta_1^2\delta_2^2}\frac{1}{f^2}\left\{1+\sqrt{\pi}\frac{\alpha f}{\beta}\,\mathrm{Re}[\Gamma T w((i\alpha/2\beta)\mu_{21}T)]+\frac{\alpha^2f^2}{\beta}|\Gamma T|^2\frac{\sqrt{\pi}}{2}\int_0^\infty dz\,e^{-\beta^2z^2}e^{-\alpha\mu_{21}^*Tz}w((i\alpha/2\beta)(\mu_{21}T+3\alpha_z))\right\},\tag{5}$$

where $\alpha^2=4/\{(k_suT)^2+12\}$, $\beta^2=\frac{3}{2}\alpha^2+1$, $\mu_{21}=[\Gamma_{21}+i(\delta_2-\delta_1)]$, and $w(z)$ is related to the complex error function by $w(z)=\exp(-z^2)\{1-\mathrm{erf}(-iz)\}$. The quantity u is the most probable speed of the sodium atoms.

A series of theoretical curves of intensity versus δ_2 is shown in Fig. 5 for $\delta_1/2\pi=-255$ GHz ($f=2$), $k_su/2\pi=1.22$ GHz, $T=0.075$ ns, and several values of the pressure. In obtaining the curves in Fig. 5, we used collision parameters $\Gamma_{10}/2\pi=11.3\pm0.4$ MHz/Torr, and $\Gamma_{20}/2\pi=39.2\pm4.6$ MHz/Torr taken from the literature[9] (collisional shifts are neglected and all values are quoted at 20 °C). The value of $\Gamma_{21}/2$ for the $3P_{1/2}$-$4D$ transition is 36.2 ± 2.1 MHz/Torr,[9] but no data are available for Γ_{21} for the $3P_{3/2}$-$4D$ transition. To fit the high-pressure data we took $\Gamma_{21}/2\pi=1.14\Gamma_{21}/2\pi=41.4\pm2.4$ MHz/Torr which leads to a value $y=\Gamma/\Gamma_{21}=0.23\pm0.17$. The distortion caused by the δ_2^{-2} dependence is clearly seen at high pressures where $\Gamma_{21}/|\delta_1|$ is no longer negligibly small. The curves are normalized such that the nonresonant background contribution is unity at $\delta_2=\delta_1$.

The theoretical ratio r of resonant to nonresonant signal amplitudes at $\delta_2=\delta_1$ is shown in Fig. 4 as a function of pressure for $T=0.075$ and 5.0 ns. The $T=5.0$ ns curve approximates the cw limit. Its departure at low pressure from the constant value of r predicted by Eq. (4) is due to the fact that the effects of atomic motion cannot be neglected [as we assumed in deriving (4)] for pressures where $\Gamma_{21}<k_su$. It is seen in Fig. 4 that the data are *not* consistent with the value $T=5.0$ ns (and, consequently, not consistent with a cw theory). On the other hand, the data agree rather well with a value $T=0.075$ ns. On can conclude that the appropriate temporal pulse width to use in Eq. (5) is some effective laser coherence time and not the actual pulse duration $T_L\simeq5$ ns. Preliminary experiments one one- and two-photon absorption give linewidths that are consistent with pulse excitation with pulses whose temporal width is of order 0.075 ns.

An independent check of our results would be provided by a measure of the spectrum of the emitted light. The spectrum, calculated as the Fourier transform of ρ_{21}, consists of two terms. First, there is a contribution from the four-wave mixing interaction which is centered at $\omega=2\Omega_2-\Omega_1$ with width T^{-1}. Second there is the contri-

bution from the resonant, collision-induced signal, which is the *product* of one term centered at $\omega=2\Omega_2-\Omega_1$ with width T^{-1} and of another centered at the atomic frequency $\omega=\omega_{21}$ with width $\simeq\max(\Gamma_{21},k_v u)$. For $k_v uT<1$ and $\Gamma_{21}T<1$, the resonant component can be separated spectrally from the nonresonant one. An experimental verification of the spectrum, which could not be performed with the current apparatus, is envisioned for the near future.

This work is supported by the U.S. Office of Naval Research and a Centre National de la Recherche Scientifique–National Science Foundation International Grant No. INT-84-13300. We should like to thank G. Grynberg for helpful suggestions throughout the progress of this work.

---

[a]Permanent address: Physics Department, New York University, New York, NY 10003.

[1]For a general review of this subject area, see *Photon-Assisted Collisions and Related Topics*, edited by N. K. Rahman and C. Guidotti (Harwood Academic, Chur, Switzerland, 1982), and J. Phys. (Paris), Colloq. **46**, C1 (1985).

[2]For a review of the use of so-called "optical" collisions to create magnetic-state coherences, see K. Burnett, Comments At. Mol. Phys. **13**, 179 (1983), and Phys. Rep. **118**, 339 (1985). For creation of magnetic-state coherence in so-called radiative collisions, see P. R. Berman, Phys. Rev. A **22**, 138, 1848 (1980); A. Debarre, J. Phys. B **15**, 1693 (1982).

[3]N. Bloembergen, H. Lotem, and R. T. Lynch, Jr., Indian J. Pure Appl. Phys. **16**, 151 (1978); Y. A. Prior, A. R. Bogdan, M. Dagenais, and N. Bloembergen, Phys. Rev. Lett. **46**, 111 (1981); A. M. Bogdan, M. Downer, and N. Bloembergen, Phys. Rev. A **24**, 623 (1981). For a recent, excellent review of this subject, see L. Rothberg, "Progress in Optics" (to be published).

[4]P. R. Berman and E. Giacobino, Phys. Rev. A **28**, 2900 (1983); P. R. Berman, Phys. Rev. A **29**, 3234 (1984).

[5]D. DeBeer, L. G. Van Wagenen, R. Beach, and S. R. Hartmann, Phys. Rev. Lett. **56**, 1128 (1986).

[6]As the collision rates approach zero, the second term in Eq. (2) must be modified to include effects of atomic motion and spontaneous decay. When this is done, it is found that, even at $\delta_{21}=0$, the second term vanishes and the collision rates go to zero.

[7]This fifth-order collisional term is to be distinguished from purely field saturation terms [see, for example, H. Friedmann and A. D. Wilson-Gordon, Phys. Rev. A **26**, 2768 (1982); B. Dick and R. M. Hochstrasser, J. Chem. Phys. **75**, 133 (1983); G. S. Agarwal and N. Nayak, Phys. Rev. A **33**, 391 (1986)] which are negligible in our experiment.

[8]Phase matiching can also be achieved by using a nonplanar geometry [see Y. Prior, Appl. Opt. **19**, 1741 (1980)] even when $\delta_1=-2\delta_2'$, which is impossible for the collinear geometry. Since this would allow a value $f\sim\infty$, it might provide a useful method for enhancing the ratio of resonant to nonresonant signal.

[9]Values are taken from the article of Allard and Kielkopf [N. Allard and J. Kielkopf, Rev. Mod. Phys. **54**, 1103 (1980)].